

Accommodation at Deformation Twins in bcc Crystals

S. MAHAJAN

The accommodation processes occurring at terminating twins, twin intersections and grain boundary-twin interactions are reviewed. It is shown that in the three situations, accommodation by slip and twinning can occur. Occasionally, microcracking is observed at a $\langle 110 \rangle$ twin intersection and a grain boundary-twin intersection. Argument is developed to reconcile these two sets of observations.

1. INTRODUCTION

DEFORMATION twins constitute homogeneously sheared regions where strains are very localized. It is therefore relatively easy to visualize that stress concentration must develop in the matrix if twin growth is obstructed. In a polycrystalline metal and alloy undergoing deformation by slip and twinning, this situation could arise when: i) a twin ceases to grow inside the lattice, ii) twins with nonparallel shear vectors intersect, and iii) a twin impinges on a high angle grain boundary. It is the objective of this paper to review the available experimental evidence concerning the accommodation processes occurring under these distinct situations and to reconcile these observations with those where twins have been identified as a source for crack nucleation.

2. ACCOMMODATION AT TERMINATING TWINS

Slip bands emanating from tips of $1/6 \langle 111 \rangle [11\bar{2}]$ twins terminating inside a crystal have been observed by several investigators.¹⁻⁶ Some of the typical examples are reproduced in Figs. 1 and 2. It is clear from Fig. 1 that the termination of twin x , lying on the $(1\bar{2}1)$ plane, has resulted in slip on the $(\bar{1}01)$, (011) and (110) planes. Another example giving a clear demonstration of the occurrence of slip ahead of a terminating twin is shown in Fig. 2. A twin ends up within the crystal at A , but it causes displacement of a sub-boundary at B which is exactly in line with the twin.

Recently, the crystallographic features of twins and of associated slip in Mo-35 at. pct Re alloy have been correlated by means of transmission electron microscopy.^{6,7} Figure 3 shows an example of a twin that stops propagating within the crystal. It is evident that the stress concentration which is likely to exist at the twin tip is accommodated by slip occurring ahead of the twin. Furthermore, the observed variation in the background intensity on either side of the dislocation image

suggests that the slipped region consists of dislocations of both signs.

Electron diffraction results coupled with trace analysis show that T_1 and slip band lie on the $(2\bar{1}1)$ plane. Since the slip dislocations are in contrast for $g = 110$ and invisible for $g = \bar{1}10$, the possible Burgers vectors are $\pm 1/2 [11\bar{1}]$ and $\pm 1/2 [1\bar{1}1]$. Combining the two preceding assessments, the activated glide system must be $\pm 1/2 [11\bar{1}](2\bar{1}1)$.

It may be emphasized that emissary slip bands need not always be present at terminating twins. The evolution of slip structures appears to depend on the thickness of twins, which in turn determines the magnitude of stress concentration, and microstructure. These aspects have been well documented by the recent work of Green and Cohen.⁸ In particular, they have shown that thin "pseudo" twins in ordered Fe-Be alloys do not yield accommodation structures.

Three proposals^{1,2,4} have been advanced to rationalize the origin of slip ahead of terminating twins, the most detailed being that of Sleeswyk.² Hull¹ visualizes that three $1/6 \langle 111 \rangle$ twinning partials of screw orientation could, after cross-slipping, coalesce to form $1/2 \langle 111 \rangle$ dislocations. These dislocations could glide away from the twin tips and produce glide bands. Thus the features observed in Fig. 1 could evolve by the cross slip of $1/2 [111]$ dislocations, gliding on the $(1\bar{2}1)$ twin plane, onto the (011) and (110) planes. Furthermore, after the occurrence of cross slip, noncoherent twin boundary still has to be described in terms of the dislocation formalism. It has to be invoked that the total Burgers vector of these structurally-necessary dislocations is zero.

According to Sleeswyk,² emissary dislocations are created by the dissociation of every third $1/6 \langle 111 \rangle$ twinning partial, bounding the noncoherent twin boundary, into a $1/2 \langle 111 \rangle$ glide dislocation and $1/3 \langle 111 \rangle$ partial. For every two $1/6 \langle 111 \rangle$ twinning partials there exists a $1/3 \langle 111 \rangle$ complementary twinning dislocation in the interface, and consequently the resultant boundary has no long range stress field associated with it and thus has a low energy. This is visualized to be the driving force for the dissociation reaction, even though it is energetically unfavorable. Furthermore, the emissary array consisting of $1/2 \langle 111 \rangle$ slip dislocations glides ahead of the propagating twin and produces a homogeneous shear equivalent to the twinning shear. It has been shown that in Fe the boundary could start

S. MAHAJAN is Member of the Technical Staff at Bell Laboratories, Murray Hill, NJ 07974.

This paper is based on a presentation made at a symposium on "The Role of Twinning in Fracture of Metals and Alloys" held at the annual meeting of the AIME, St. Louis, Missouri, October 15-19, 1978, under the sponsorship of the Mechanical Metallurgy Committee of The Metallurgical Society of AIME.

dissociating when the twin reaches a thickness of $\sim 40\text{\AA}$.

Since the modified noncoherent twin boundary has a zero net displacement vector, it cannot glide under an applied stress. It is therefore difficult to comprehend how noncoherent interfaces could move after the dissociation. It is envisaged that the emissary array begins to form only when the twin stops propagating.

An alternative mechanism involving homogeneous nucleation of $1/2 \langle 111 \rangle$ shear loops on every third $\{11\bar{2}\}$ plane ahead of the stopped twin could also explain the experimental observations.⁴ When stressed, these loops expand and subsequently interact with the twinning partials. The resulting situation at the noncoherent twin boundary is analogous to the one visualized by Sleswyk.² It appears, however, rather fortuitous to expect these loops to nucleate in such a regular manner.

The observed crystallographic relationship between T_1 and the glide dislocations shown in Fig. 3 can be

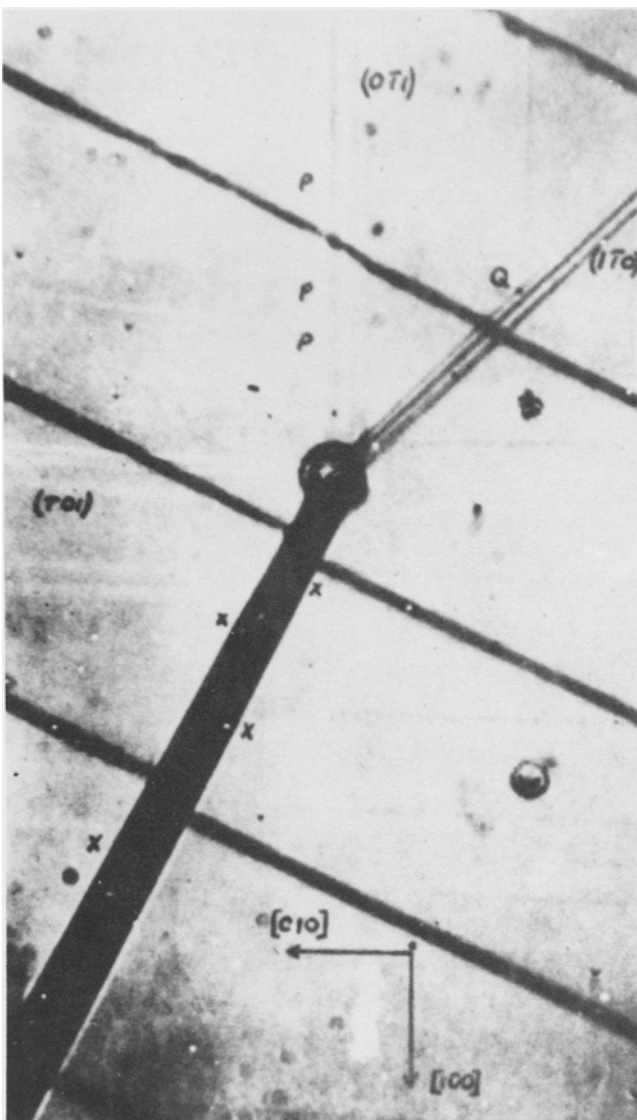


Fig. 1—Tip of a $(1\bar{2}1)$ $[111]$ deformation twin showing glide bands produced by slip on $(\bar{1}01)$, $(0\bar{1}1)$ and $(1\bar{1}0)$ planes. The dark diagonal lines are line profiles which are homogeneously displaced across the twin. (After Hull.¹)

rationalized according to the hypotheses of Hull¹ and Sleswyk.² However, the presence of positive and negative dislocations on the same side of the twin is at variance with the expected behavior, but these features could evolve as follows. As a shear loop glides away from the matrix-twin interface, a small segment may undergo multiple cross glide. This process results in nonscrew, jogged dislocations that are opposite in nature and located on planes which are parallel to the composition plane of the twin. Both types of dislocations are equally effective in accommodating the twinning strain because they produce identical strains by gliding in opposite directions. One type of dislocations would have to glide through the twin. It is envisaged that this should occur readily because they can be easily incorporated into the twin.⁹

3. ACCOMMODATION AT TWIN INTERSECTIONS

Based on the line of intersection between a crossing and a crossed twin, a convenient classification for different twin intersections can be developed. Accordingly, five types of interactions, *i.e.* $\langle 111 \rangle$, $\langle 210 \rangle$, $\langle 110 \rangle$, $\langle 531 \rangle$ and $\langle 311 \rangle$, can occur in bcc crystals. These intersections have been investigated in detail by optical metallography^{5,12,13} and transmission electron microscopy.^{7,10,11}

Since the twinning partial bounding a noncoherent boundary of a crossing twin could either coalesce¹ or dissociate² to form slip dislocations, twin-twin intersections can be regarded as equivalent to twin-slip interactions; this equivalence was first suggested by

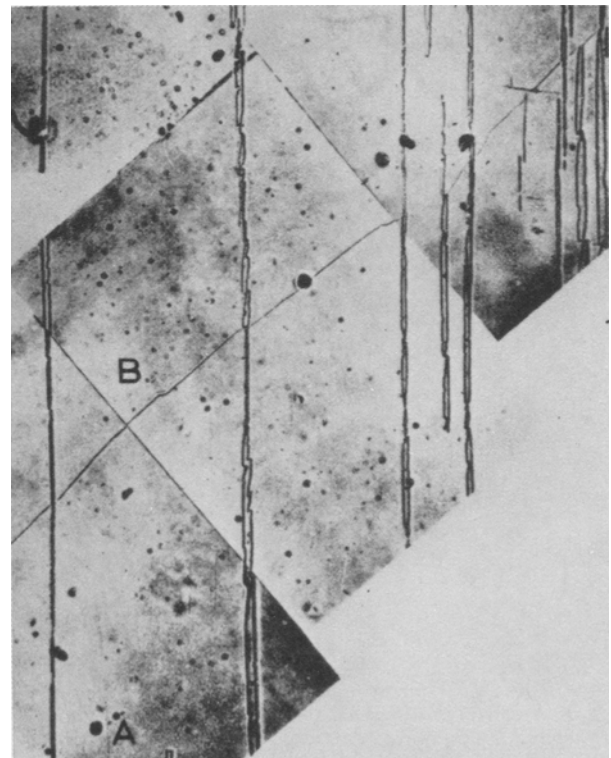


Fig. 2—Deformation twins formed in pure Fe during compression at 77 K showing the distortion of a subboundary at *B* ahead of a twin which has stopped at *A*. (After Sleswyk.²)

Sleeswyk.¹² Therefore, the procedure developed by Sleeswyk and Verbraak⁹ for the incorporation of slip dislocations into twins can be utilized to analyze twin-twin intersections.

3.1 $\langle 111 \rangle$ Intersection

In this situation, the shear vectors of the crossing and crossed twin are parallel. Consequently, this constitutes the simplest interaction that can occur. Sleeswyk and Helle¹³ have investigated in detail these intersections in α -Fe, and have shown that the formation of zigzag twin configurations can be accounted for in terms of such crossings.

Figure 4 shows an example of these crossings in an α -Fe sample deformed at a low temperature.¹³ The composition planes of twins 7A and 7B, and 12, are $(\bar{1}\bar{1}2)$ and $(1\bar{2}1)$, respectively. The twins 7A and 12 cross each other completely, whereas the twin crossing 7B-12 is a branching crossing. The latter type of crossing,

observed by transmission electron microscopy in deformed Mo-35 at. pct Re alloy is reproduced in Fig. 5(a).¹⁰ The interacting twins T_1 and T_2 , lying on the $(\bar{1}21)$ and $(2\bar{1}1)$ planes, respectively, merge into each other with little or no deformation of the adjoining matrix.

It is apparent that twins 7B and T_1 cease to widen only on those sides of the crossing twins which enclose obtuse angles. This can be understood as follows. The unidirectionality of twinning implies that by specifying the twinning plane and the sense of twinning shear for one of the twins, the twinning elements for the remaining twinning systems can be fixed. Assuming that T_1 is caused by the $1/6 [11\bar{1}]$ slip of the successive $(\bar{1}21)$ planes, T_2 could then only result from $1/6 [11\bar{1}]$ glide of the $(2\bar{1}1)$ planes. With these crystallographic restrictions and following the suggestions of Sleeswyk and Helle,¹³ it can be shown that only on the side which encloses an acute angle between the twin planes are the atom movements necessary for the widening of T_1 and T_2 matched and geometrically compatible. Hence on that

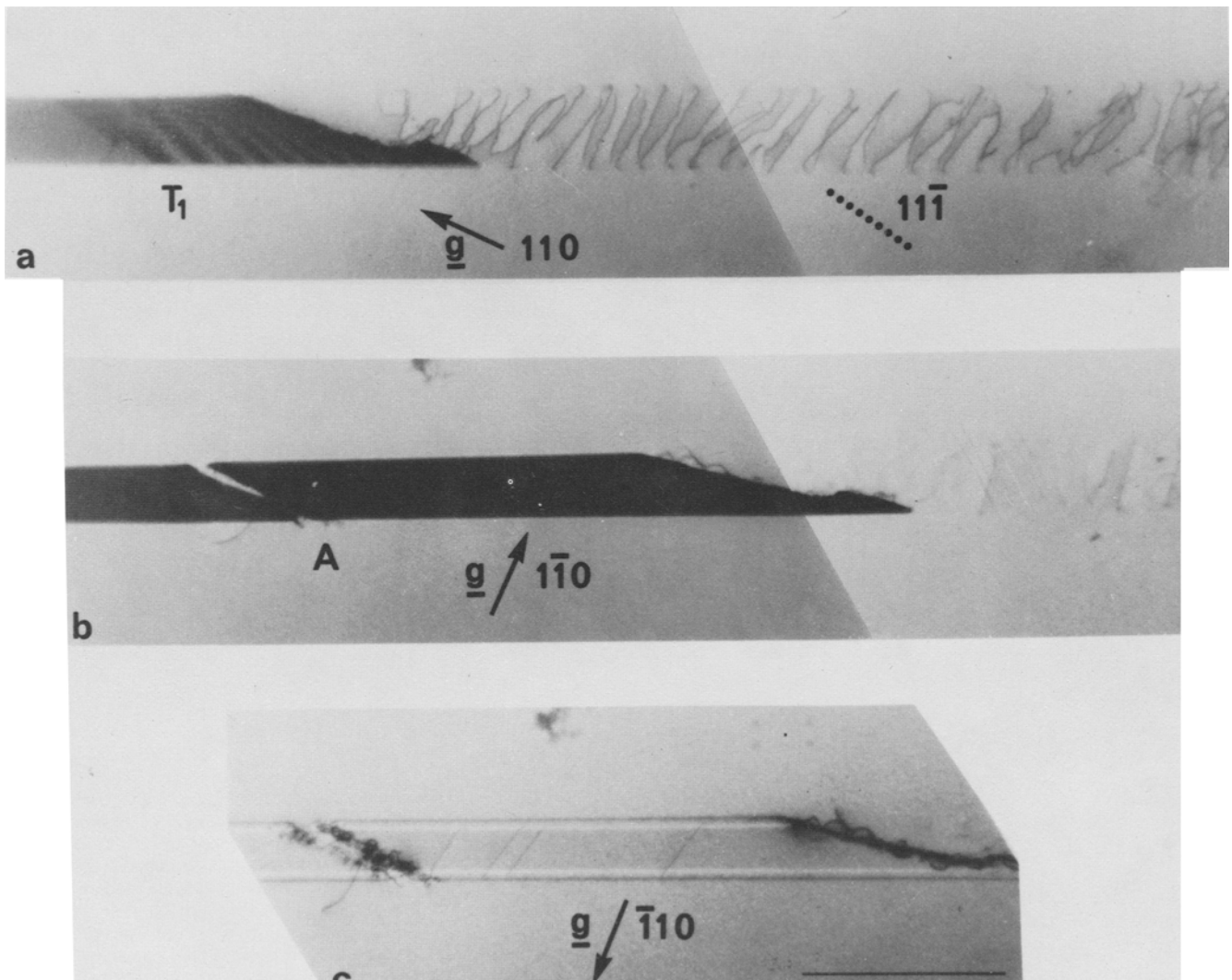


Fig. 3—Slip emanating from a twin which terminates within the crystal. The planes of the micrographs (a), (b) and (c) are $\sim(1\bar{1}5)$, $\sim(115)$ and $\sim(001)$, respectively. Dotted line in (a) refers to the projections of the $[11\bar{1}]$ vector onto the $(1\bar{1}5)$ plane. The marker represents 1 μm . (After Mahajan.⁶)

side they could widen cooperatively and thus lead to the situation which is consistent with the one shown in Fig. 5(a). The formation of massive joints only on those sides of the crossing twins enclosing acute angles in Fig. 4 can be rationalized in a similar fashion.

It appears that the twin crossing 7A-12 is accomplished by slip. To achieve that the twinning partials must coalesce or dissociate to form $1/2 \langle 111 \rangle$ dislocations at the interface of the crossed twin. Subsequently, these dislocations could glide through the crossed twin on a plane which is continuation of the crossing twin. After crossing, the glide dislocations could dissociate to form a twin on the exit side.

Levasseur⁵ and Kounicky¹¹ have reported detwinning on a plane which is not parallel to the composition plane of the crossed twin. This is an interesting observation, but it is not possible to rationalize these results in terms of the foregoing analysis.

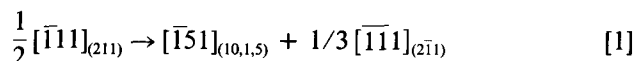
3.2 $\langle 210 \rangle$ Intersection

Figure 5(b) shows a $\langle 210 \rangle$ interaction in deformed Mo-35 at. pct Re alloy.¹⁰ Electron diffraction and single surface trace analysis showed that the composition planes of T_3 and T_4 are $(\bar{2}11)$ and (211) , respectively. Dark-field imaging also showed that the intersection of T_4 with T_3 induces slip on $(10,1,5) \parallel (2\bar{3}1)_{T_3}$ * plane of

* Subscript T_3 denotes that the indices are with respect to the T_3 reference system.

T_3 . Levasseur's⁵ observations agree with this result. He also observes that some of the $1/2 \langle 111 \rangle$ dislocations, gliding within the crossed twin, cross slip onto $\{110\}$ planes. Furthermore, slip dislocations belonging to the $1/2 [111] (231)$ slip system are observed in the lower left corner of Fig. 5(b).

Since the interaction of T_4 with T_3 induces slip on the $(10,1,5)$ plane of T_3 , the Burgers vectors of the glide dislocations must therefore be $1/6 [\bar{1}51] = 1/2 [111]_{T_3}$. These dislocations could result from the dissociation of the $1/2 [\bar{1}11]$ glide dislocations according to the following reaction:

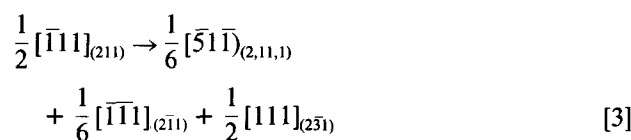
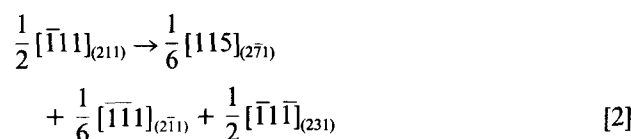


The $1/2 [\bar{1}11]$ dislocations may, in turn, originate when

the $1/6 [\bar{1}11]$ twinning partials comprising the non-coherent twin boundary of T_4 either coalesce or dissociate. At the second coherent twin interface the $1/6 [\bar{1}51]$ dislocations could dissociate into the $1/2 [\bar{1}11]$ dislocations in the matrix and the $1/3 [111]$ dislocations in the boundary. T_4 could evolve from the $1/2 [\bar{1}11]$ dislocations as detailed out previously.⁷

The decomposition reaction is energetically unfavorable, but it could occur when a sufficient number of the $1/2 [\bar{1}11]$ dislocations has piled up against the twin to relieve the stress concentration at the head of the pile-up.

The choice of glide plane in the twin is dictated by the geometrical condition that the line of intersection of T_3 and T_4 must lie in the glide plane. In the present situation, in addition to the observed glide plane, *i.e.* $(10,1,5) \parallel (2\bar{3}1)_{T_3}$, this condition is satisfied by $(2\bar{7}1) \parallel (211)_{T_3}$ and $(2,11,1) \parallel (231)_{T_3}$ planes of the twin. The decomposition reactions satisfying the crystallographic requirements can be written as shown below:



The observed activation of the $1/2 [111] (2\bar{3}1)$ slip system may be accounted for in terms of Reaction [3].

Besides the geometrical restriction outlined above, two other factors may govern the activation of a geometrically compatible glide plane: i) the magnitude of resolved shear stress on a slip plane within the twin; ii) energetics of the dissociation reactions. Since the observed glide plane makes the smallest angle with the composition plane of T_4 , it is likely to carry a higher resolved shear stress than the other two choices. Also, based on energetics Reaction [1] is more likely to occur than Reactions [2] and [3]. Therefore, Reaction [1] is favored on both of these accounts. However, the reason for the occurrence of Reaction [3] is not clear.

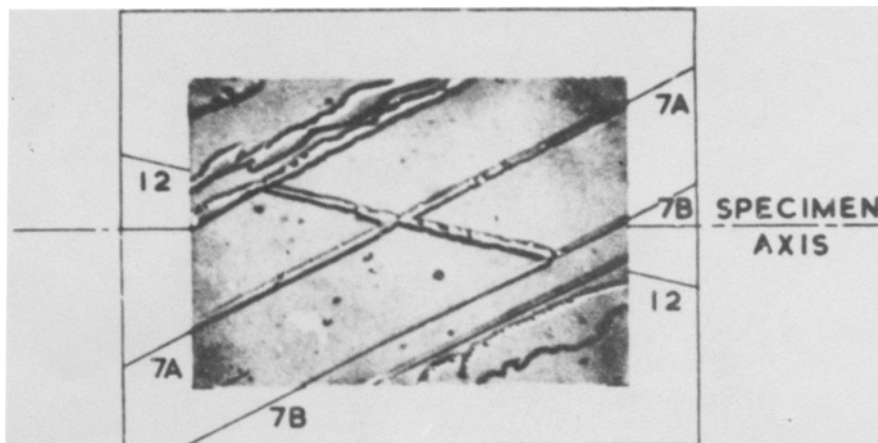


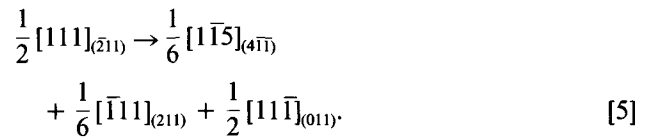
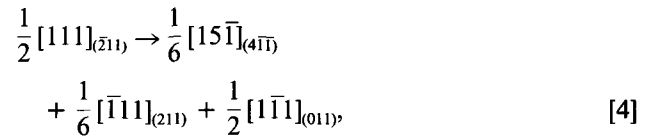
Fig. 4—Micrograph of the surface of an α -Fe specimen after 9.2 pct tensile deformation in liquid oxygen. Electro polished, Magnification 378 times. (Reduced approximately 70 pct for reproduction.) The twins 7A and 12 crossed each other completely in an early stage. Later transverse growth took place only on those sides of the crossing twins which enclose acute angles. The twin crossing 7B-12 is a branching crossing. (After Sleswyk.¹³)

3.3 $\langle 110 \rangle$ Intersection

A situation observed after the occurrence of a $\langle 110 \rangle$ intersection in deformed Mo-35 at. pct Re alloy is reproduced in Fig. 5(c). Twins T_5 and T_6 , lying on the (211) and $(\bar{2}11)$ planes, respectively, interact with each other resulting in slip bands S_1 and S_2 . It has been shown that the glide systems constituting S_1 are $1/2 [11\bar{1}]_{(011)}$ and $1/2 [1\bar{1}\bar{1}]_{(011)}$. Furthermore, on the basis of the single-surface trace analysis it is concluded that $(\bar{2}11)$, $(\bar{2}13)$, $(2\bar{1}3)$ and $(2\bar{1}1)$ are the only possibilities for the habit plane of S_2 . The preceding observations are consistent with that of Levasseur.⁵ (See his Fig. 11.)

The observed crystallographic features can be rationalized if the $1/2 [111]$ dislocations, resulting by either the coalescence or the decomposition of the

twinning partials, dissociate according to the following reactions:



S_1 's could form when the $1/2 [1\bar{1}\bar{1}]$ and $1/2 [11\bar{1}]$ dislocations glide away from the intersection zone on the (011) planes. The $1/6 [1\bar{1}5]$ and $1/6 [15\bar{1}]$ dislo-

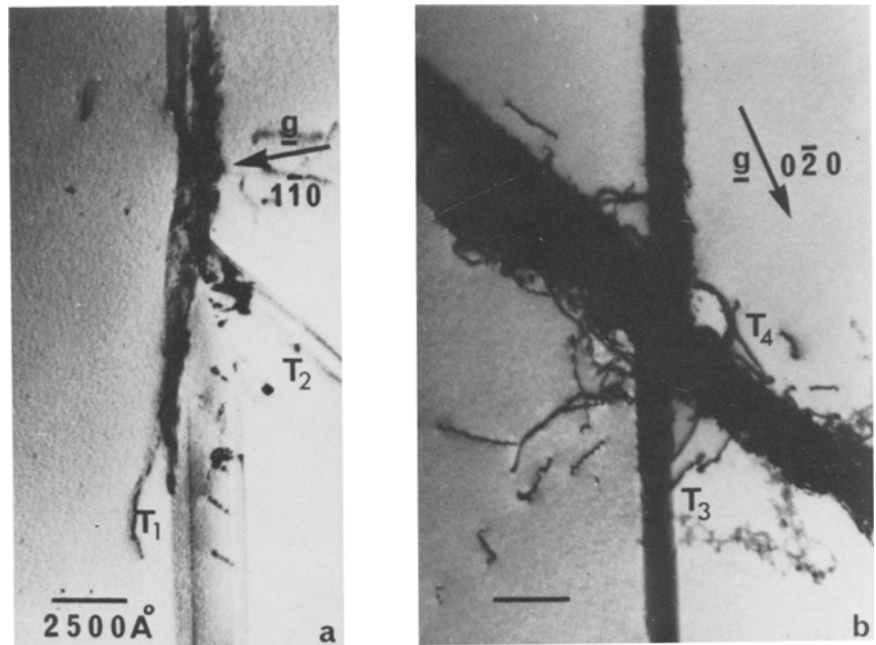
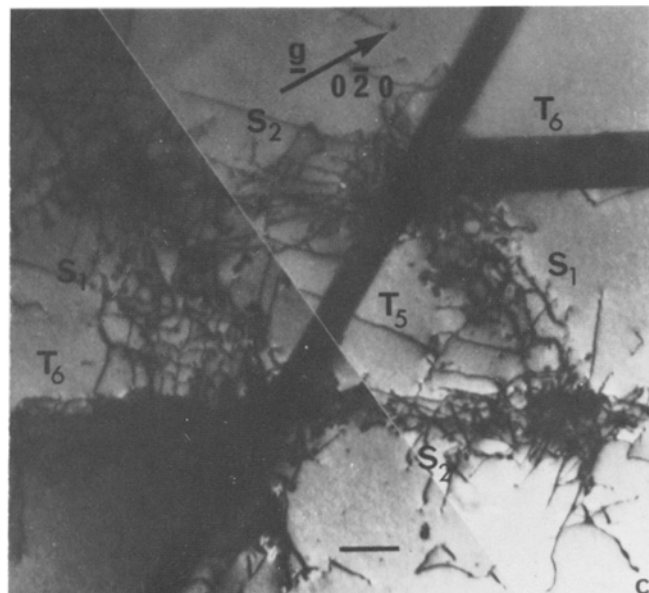


Fig. 5—Various twin-twin interactions observed in deformed Mo-35 at. pct Re alloy specimens. The planes of the micrographs (a), (b) and (c) are $\sim(115)$, $\sim(001)$ and $\sim(001)$, respectively. (After Mahajan.¹⁰) The markers in (b) and (c) represent 2500\AA

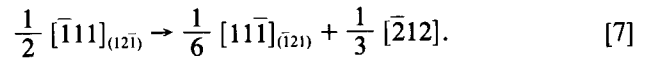


cations could dissociate at the exit side, and S_2 's could form by slip of the resulting segments. The absence of well-developed S_1 's on the exit side suggests that the $1/2 [\bar{1}\bar{1}\bar{1}]$ and $1/2 [\bar{1}\bar{1}\bar{1}]$ dislocations may have cross-slipped onto the $(\bar{2}13)$ and $(2\bar{1}\bar{1})$ planes, and therefore, in addition to the $1/2 [111]$ dislocations, may contribute to the formation of S_2 's.

In addition to the $(4\bar{1}\bar{1}) \parallel (011)_T$ plane the line of intersection of T_5 and T_6 also lies in the $(255) \parallel (211)$ plane. The $1/2 [111]$ dislocations could then be incorporated into the twin by the following reaction:

Based on energetics Reaction [6] is more likely to occur than Reactions [4] and [5], and could be occurring simultaneously. However, it is not possible to present evidence in support of Reaction [6] because the slip plane in T_5 could not be ascertained experimentally.

Figure 6 is an optical micrograph of a $\langle 110 \rangle$ intersection observed in an α -Fe single crystal deformed at liquid nitrogen temperature.⁵ It appears that the $(12\bar{1})$ - $(\bar{1}\bar{2}1)$ interaction induces microcracking. Levasseur⁵ has hypothesized that the $1/2 [\bar{1}\bar{1}\bar{1}]$ dislocations, resulting either from the coalescence or the decomposition of $1/6 [\bar{1}\bar{1}\bar{1}]$ twinning dislocations, could dissociate according to the following reactions:



The formation of $1/3 [\bar{2}12] \equiv [010]_T$ dislocations may result in cleavage on the (010) planes as first suggested by Cottrell.¹⁴

3.4 $\langle 531 \rangle$ Intersection

Figure 7 shows a $\langle 531 \rangle$ intersection in a deformed Mo-35 at. pct Re alloy. The interaction of twins T_2 and T_3 , having the (211) and $(\bar{1}\bar{2}1)$ habits, results in a slip band S_1 and a few dislocations W . It has been shown that S_1 is due to the $1/2 [11\bar{1}] (\bar{1}\bar{2}1)$ glide, whereas the Burgers vector of dislocations W is $1/2 [111]$. Furthermore, by dark-field imaging it has been ascertained that during the intersection, T_2 deforms by slip. However, the glide plane within T_2 could not be determined experimentally.

Again, the origin of various crystallographic features during the intersection can be rationalized if the $1/2 [11\bar{1}]$ dislocations, resulting by either the coalescence or the dissociation of the twinning partials, dissociate at

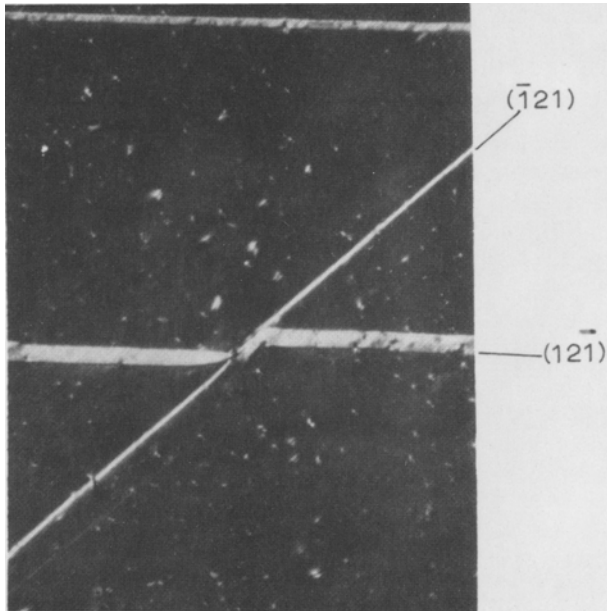


Fig. 6—A $\langle 110 \rangle$ twin intersection observed in an α -Fe single crystal deformed at liquid nitrogen temperature. This intersection induces microcracking. (After Levasseur.⁵)

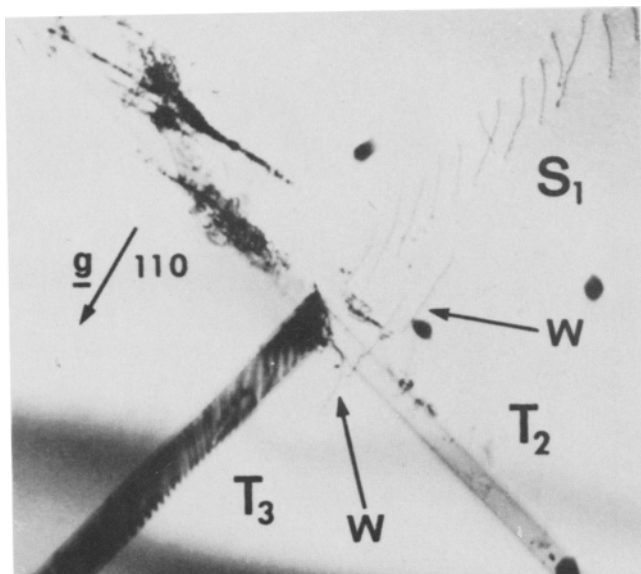


Fig. 7—An example of a $\langle 531 \rangle$ twin intersection observed in a deformed Mo-35 at. pct Re alloy. The plane of the micrograph is $\sim(001)$. (After Mahajan.¹⁰)

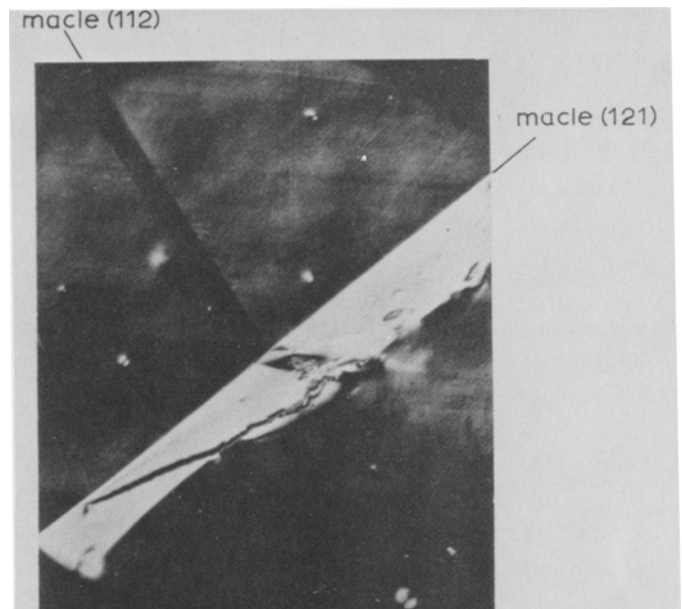
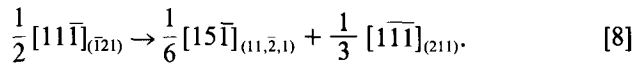


Fig. 8—An optical micrograph showing a $\langle 311 \rangle$ twin intersection observed in an α -Fe sample deformed at liquid nitrogen temperature. (After Levasseur.⁵)

the coherent boundary of T_2 according to the following reaction.

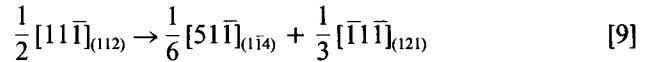


The $1/6 [15\bar{1}]$ dislocations could glide through T_2 on the $(11,2,1) \parallel (132)_{T_2}$ planes. They could subsequently dissociate at the exit side, and S_1 could form by glide of the $1/2 [11\bar{1}]$ segments. However, the origin of dislocations W is not clear.

3.5 $\langle 311 \rangle$ Intersection

Levasseur has investigated in detail this type of interaction in deformed α -Fe crystals. Figure 8 depicts one of the observed situations. As a result of the (121) - (112) twin intersection, slip occurs on the $(1\bar{1}4) \parallel (01\bar{1})_T$ planes of the twin. Some of the dislocations

appear to cross glide onto the $(2\bar{5}5) \parallel (\bar{1}\bar{1}2)_T$ planes within the (121) twin. The observed features have been rationalized in terms of the following dislocation reaction:



4. ACCOMMODATION AT GRAIN BOUNDARY-TWIN INTERSECTIONS

There are very few studies where the interaction of twins with grain boundaries has been evaluated. The observations of Gilbert *et al*¹⁵ indicate that in W, Cr, and Mo a grain boundary may part locally when a twin impinges upon it. In contrast the studies of Spreadborough *et al*¹⁶ and Mahajan^{7,17} show that the stress concentration existing in the vicinity of the interaction region is generally relaxed by slip in the two grains, but

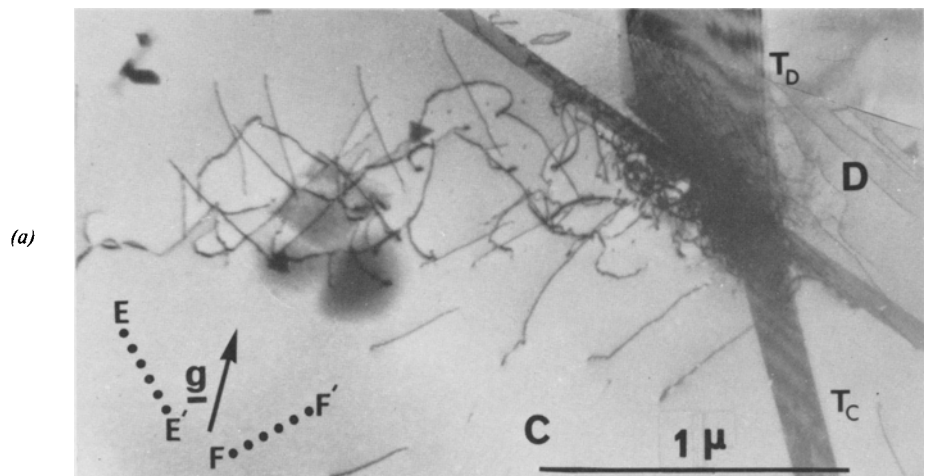
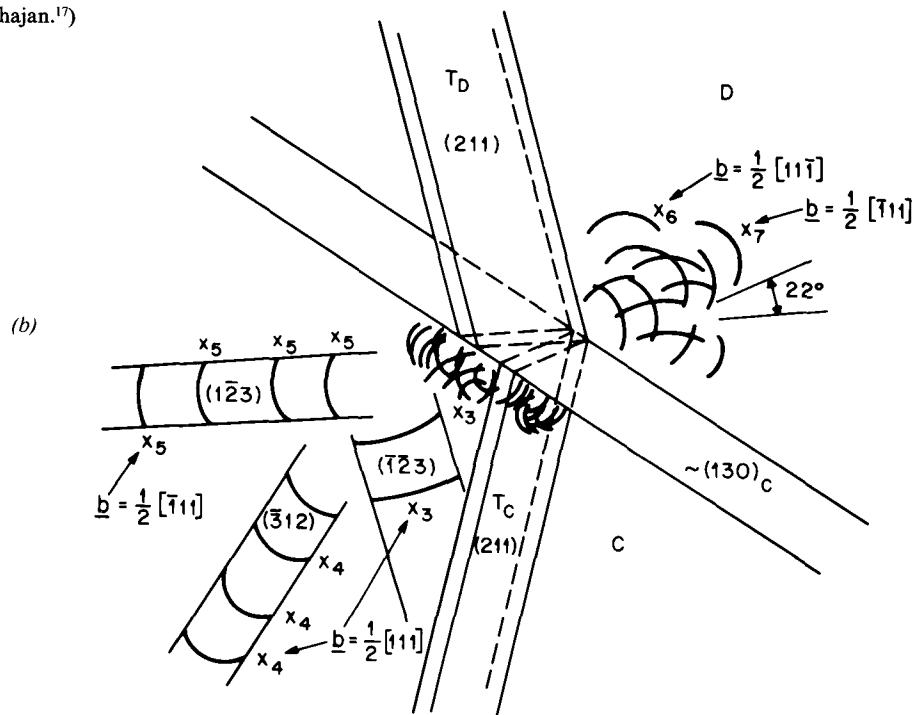


Fig. 9—(a) Electron micrograph illustrating the interaction of a twin with a grain boundary in deformed Mo-35 at. pct Re alloy. The plane of the micrograph is $\sim(001)_C$. EE' and FF' refer to the projections of the $[\bar{1}\bar{1}\bar{1}]$ and $[\bar{1}\bar{1}\bar{1}]$ and $[111]$ and $[111]$ directions onto the $(001)_C$ plane. (b) Schematic of the situation shown in (a); the crystallography of various features is identified on the figure. (After Mahajan.¹⁷)



occasionally twinning also intervenes; in no case are microcracks seen at the grain boundary-twin intersections.

Figure 9(a) shows an example of a grain boundary-twin interaction observed in a deformed Mo-35 at. pct Re alloy specimen.¹⁷ A twin T_C interacts with a boundary separating grains C and D , resulting in slip bands within grain C and a twin T_D and slip dislocations in grain D . The crystallography of various substructural features has been ascertained and these results are summarized in Fig. 9(b). It is evident that the lines of intersection of T_C and T_D with the boundary plane have an angular separation of ~ 22 deg. This implies that the $(211)_C$ and $(211)_D$ planes are not symmetrically disposed about the boundary plane. Thus the deformation on the $[\bar{1}11](211)_C$ and $[\bar{1}11](211)_D$ systems alone will produce strain incompatibility at the boundary. It is suggested that the additional deformation systems observed in grains C and D come into operation to produce a compatible strain situation at the boundary.

The development of the crystallographic features can again be rationalized by invoking the formation of $1/2 \langle 111 \rangle$ dislocations from partials bounding a noncoherent twin boundary. For conciseness, the discussion will be limited to the evolution of T_D . Since the habit planes of T_C and T_D do not intersect the boundary along a common line, the $1/2 [\bar{1}11]_C$ dislocations, resulting by either the decomposition or the coalescence of the twinning partials, may dissociate into glissile and sessile components in the boundary. The glissile segments, after realignment, could dissociate to produce $3 \times 1/6 [\bar{1}11]_D$ dislocations. The glide of these dislocations on the $(211)_D$ planes may lead to the formation of T_D . The development of other crystallographic features can be explained in a similar fashion.

5. TWINNING AND CRACK NUCLEATION

The experimental evidence reviewed in the preceding sections shows that in all situations where stress concentration must develop when twin growth is obstructed, accommodation by slip and twinning can occur. However, occasionally microcracking is observed at a $\langle 110 \rangle$ twin intersection and a grain boundary-twin interaction. From the present results, it is difficult to ascertain what factors govern the choice between crack-free and crack-containing accommodation. It is tempting to speculate that, in addition to a suitably oriented stress, the rate of twin growth may be equally important. The growth rate, in turn, determines the shape of noncoherent twin boundary and the resulting stress concentration. The higher the growth rate, the more likely it is for microcracks to nucleate. This is

inferred because the higher growth rate requires that the accommodation processes occur at a comparable rate. Since slip in bcc crystals is highly strain-rate or temperature sensitive, it is conceivable that locally the fracture stress is reached before accommodation by slip can occur.

6. CONCLUSIONS

If a polycrystalline material deforms simultaneously by slip and twinning, stress concentrations could develop at terminating twins, twin intersections and grain boundary-twin interactions. It is shown that in the three situations, accommodation by slip and twinning can occur. Occasionally, microcracking is observed at a $\langle 110 \rangle$ twin intersection and a grain boundary-twin intersection. It is argued that microcracking occurs when twins propagate at a high rate. The higher propagation rate, in turn, affects the shape of the noncoherent twin boundary and thus the resulting stress concentration. It is conceivable that at these high rates, the fracture stress is reached locally before accommodation by slip can occur. Based on this study it appears that deformation twins do not play a major role in the nucleation of fracture in bcc crystals.

ACKNOWLEDGMENT

The author would like to thank G. Y. Chin for his constructive comments on the manuscript.

REFERENCES

1. D. Hull: *Acta Metall.*, 1961, vol. 9, pp. 909–12.
2. A. W. Sleeswyk: *Acta Metall.*, 1962, vol. 10, pp. 705–25.
3. E. Votava and A. W. Sleeswyk: *Acta Metall.*, 1962, vol. 10, pp. 965–70.
4. D. Hull: *Deformation Twinning*, R. E. Reed-Hill, J. P. Hirth, and H. C. Rogers, eds., pp. 121–55, Gordon and Breach, New York, 1964.
5. J. Levasseur: *Mater. Sci. Eng.*, 1969, vol. 4, pp. 343–52.
6. S. Mahajan: *J. Phys. F: Met. Phys.*, 1972, vol. 2, pp. 19–23.
7. S. Mahajan: *Acta Metall.*, 1975, vol. 23, pp. 671–84.
8. M. L. Green and M. Cohen: *Acta Metall.*, 1979, vol. 27, pp. 1523–38.
9. A. W. Sleeswyk and C. A. Verbraak: *Acta Metall.*, 1961, vol. 9, pp. 917–27.
10. S. Mahajan: *Philos. Mag.*, 1971, vol. 23, pp. 781–94.
11. J. Kounický: *Phys. Status Solidi (9)*, 1970, vol. 2, pp. 455–62.
12. A. W. Sleeswyk: *Acta Metall.*, 1964, vol. 12, pp. 669–73.
13. A. W. Sleeswyk and J. N. Helle: *Acta Metall.*, 1961, vol. 9, pp. 344–51.
14. A. H. Cottrell: *Trans. TMS-AIME*, 1958, vol. 212, pp. 192–203.
15. A. Gilbert, G. T. Hahn, C. N. Reid, and B. A. Wilcox: *Acta Metall.*, 1964, vol. 12, pp. 754–55.
16. J. Spreadborough, D. Langheinrich, E. Anderson, and D. Brandon: *J. Appl. Phys.*, 1964, vol. 35, pp. 3585–87.
17. S. Mahajan: *Acta Metall.*, 1973, vol. 21, pp. 255–60.